

Catalytic Cavitands

An Introverted Bis-Au Cavitand and Its Catalytic Dimerization of Terminal Alkynes

Naoki Endo,^[a] Mao Kanaura,^[a] Michael P. Schramm,^[b] and Tetsuo Iwasawa*^[a]

Abstract: A preparative synthesis of an inwardly oriented phosphoramidite-Au dinuclear resorcinarene cavitand complex is described, including a description of potent catalytic abilities. The cavitand structure was determined by crystallographic analysis, which revealed that the phosphoramidite P–N bonds point outside placing the two Au atoms inside. We explored the catalytic

proclivity of the cavitand and found that it efficiently catalyzes selective and direct dimerization of terminal alkynes to afford conjugated enynes. Mixed dimerizations give rise to chemo-selective products, and macrocyclization by intramolecular dimerization are both trademark capabilities of the method.

Introduction

Natural supramolecules like enzymes integrate inwardly oriented functionalities.^[1] Proteins concentrate several functional groups of amino acids toward guest molecules to create reaction sites inside hydrophobic pockets. We know too that several proteins incorporate multiple metals that activate otherwise inert molecules inside their enclosed cavities.^[2] An additional feature is that part of the enzymatic pocket remains open so that guests can sample the space, enter and leave. Protein construction is both inspiring and daunting; atomic molecular machines, perfectly organized to perform efficient catalytic chemical transformations essential to countless biological operations.^[3] Whereas mother nature remains the teacher of such chemical transformations, we continue to be her students. Using artificial supramolecules we find similarities and new possibilities for controlled molecular catalysts that simultaneously employ principles from the fields of both supramolecular chemistry and catalysis.^[4] Although organic chemists have long sought to develop catalysts bearing inwardly oriented functional substituents within specified chemical spaces,^[5,6] such “introverted” functionalized cavitands have not yet attained the status associated with powerful synthetic platforms.^[7] Overcoming this historical drawback will likely enable cavitands to have much greater impact on the synthetic community; a properly constructed metal–cavitand hybrid may serve as a real tool for gaining insights into new modes of chemical catalysis and discovery of new transformations.^[8]

We recently reported the synthesis of an introverted phosphorus-Au species tethered to a cavitand scaffold of triquinoxaline-spanned resorcin[4]arene [Scheme 1 (a)].^[9] The arrangement of one Au atom, pointing inward and flanked by 3 aromatic walls, provided a new architecture for alkyne catalysis; both hydration and Conia–ene reactions were demonstrated using this cavitand system. We think this arrangement holds great promise for further investigations.^[10] With an interior functionality capable of acting as a supporting ligand for complexation with transition metals, new roads appear.^[11–13] These findings drove us to develop an introverted multi-metallated cavitand as an effective catalyst in organic synthesis. The real question we continue to pursue is “*can these new organometallic-cavitand hybrid frameworks enable new and potent chemical transformations?*”.

Results and Discussion

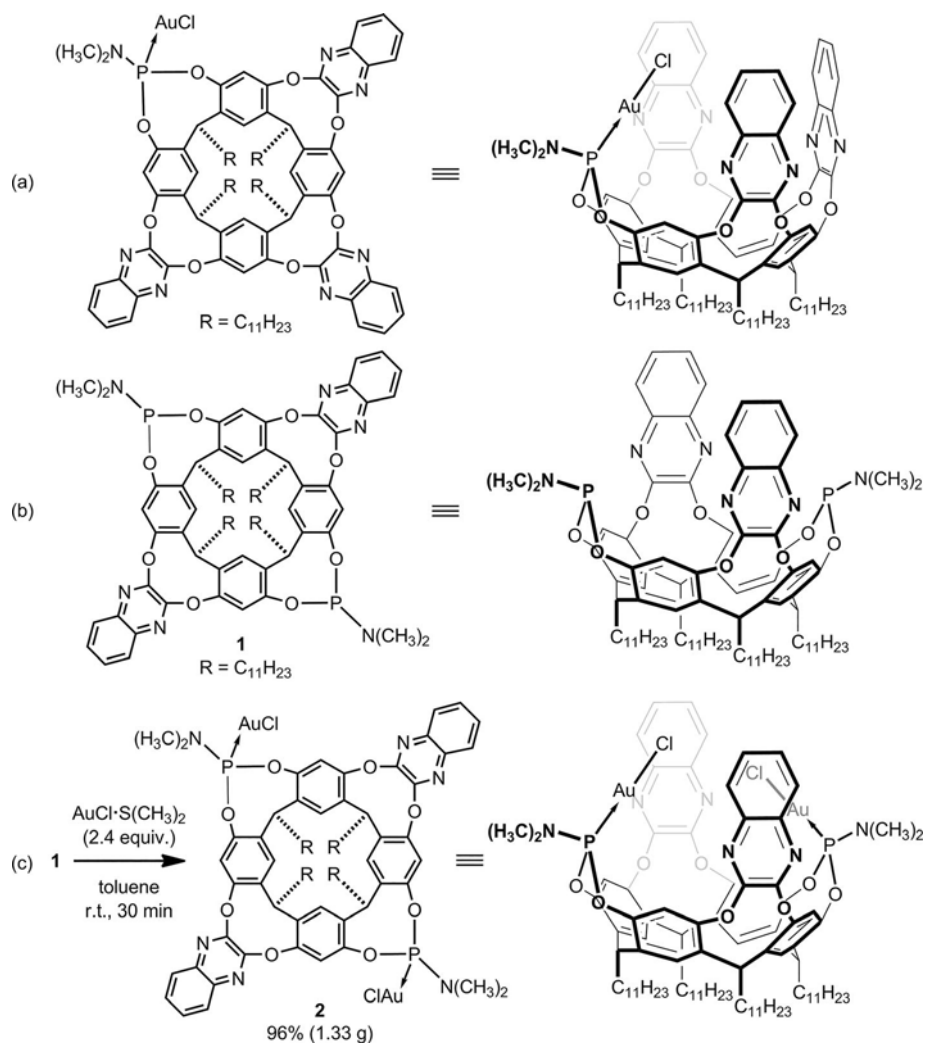
Diphosphoramidite **1** in Scheme 1 (b) was reported in 2008 by our group; **1** was readily prepared as one of three possible isomers (“in-in”, “out-out”, or “in-out”).^[14] Reaction of **1** with AuCl-S(CH₃)₂ afforded quantitative formation of bis-Au cavitand **2**, and this approach was amenable to a preparatory 1.33 g-scale of **2** [Scheme 1 (c)]. The molecular structure of **2** was determined by crystallographic analysis, which made apparent its introverted Au arrangements (Figure 1).^[15] The two quinoxaline walls flank the two metal centers. In our reported crystal structure, we find a confined molecule of CH₂Cl₂ that is sandwiched between two gold atoms and the two quinoxaline walls.^[16]

In seeking to develop a reactivity profile for **2**, we followed the examples that we had previously explored for **1**.^[9] In examining the **2**-mediated Conia–ene^[17] reaction we were surprised to find no evidence of cyclization – instead, bis-Au cavitand **2** brought two alkynes together to result in a dimerization event

[a] Department of Materials Chemistry, Ryukoku University, Seta, Otsu, Shiga 520-2194, Japan
E-mail: iwasawa@rins.ryukoku.ac.jp
<http://www.chem.ryukoku.ac.jp/iwasawa/index.html>

[b] Department of Chemistry and Biochemistry, California State University Long Beach (CSULB), 1250 Bellflower Blvd. Long Beach, Los Angeles, CA 90840, USA
<https://schrammlab.wordpress.com/>

Supporting information for this article is available on the WWW under <http://dx.doi.org/10.1002/ejoc.201600362>.



Scheme 1. (a) Mono-phosphoramidite; (b) diphosphoramidite **1**; (c) complexation of **1** with $\text{AuCl} \cdot \text{S}(\text{CH}_3)_2$ to yield **2**.

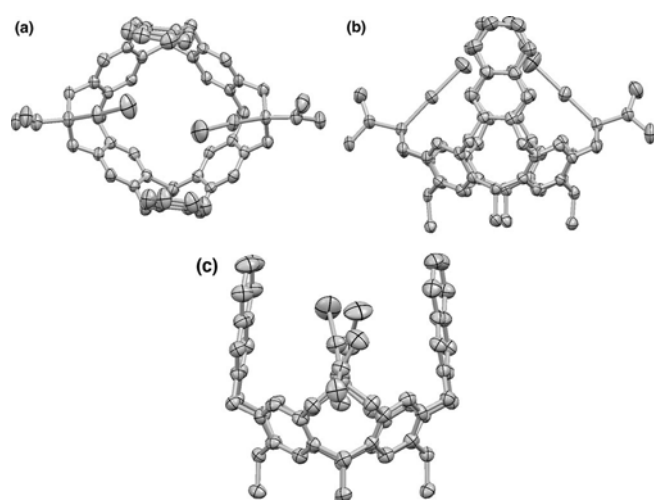
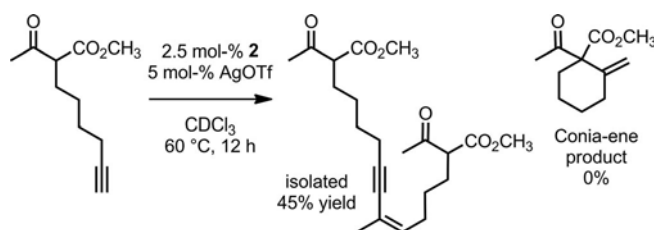


Figure 1. ORTEP drawing of **2** with thermal ellipsoids at the 50% probability level: (a) top view; (b) side view from a quinoxaline wall; (c) side view from a phosphoramidite moiety. The interior CH_2Cl_2 is deleted for ease of viewing, and hydrogen atoms are omitted for clarity.

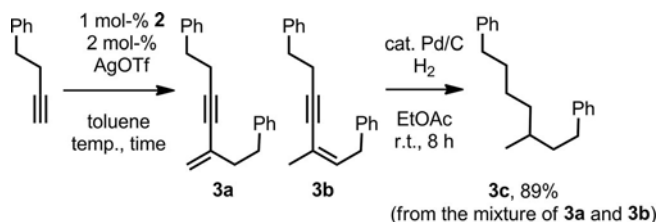
(Scheme 2). The resulting enyne was isolated as the major product in 45% yield. Initial spectroscopic data were perplexing as we were expecting a cyclohexane fragment. However, MS, COSY and NIOSY analyses allowed for a straightforward assignment.^[18]



Scheme 2. Dimerization of methyl 2-acetyloct-7-ynoate.

The significance of this result was obvious to us. Cavitand **2** has potentially important abilities; the cavitand has two inward Au atoms, and entices two reaction partners inside to carry out a coupling reaction. As multiple reaction components were used, control experiments with only Ag sources or with **2** alone failed to consume any starting material.

Encouraged by this preliminary result, we examined the dimerization of commercially available 4-phenyl-1-butyne (Scheme 3); **2** catalyzed the homo-dimerization to give a mixture of two distinguishable isomeric enynes **3a** and **3b**. Both products were labile, so the mixture was reduced to a single aliphatic molecule **3c** in 89 % yield. Interestingly, the ratios of **3a/3b** were dependent on the reaction temperature (Table 1); as the temperature was ramped from 0 °C to 105 °C, the ratios of **3a/3b** almost completely inverted from ca. 100:0 to 7:93. However, complete mechanistic details for this temperature-based isomerization are not yet fully known.



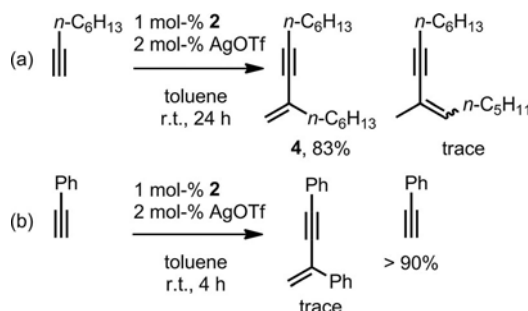
Scheme 3. Cavitand **2** catalyzed dimerization of 4-phenyl-1-butyne.

Table 1. Temperature-dependent ratios of **3a/3b** produced as in Scheme 3.^[a]

Entry	Temp. [°C]	Time [h]	Yield [%] ^[b]	Ratio of 3a/3b ^[c]
1	0	24	53	ca. 100:0
2	r.t.	24	59	93:7
3	45	2	82	91:9
4	65	3	67	47:53
5	105	2	48	7:93

[a] Conditions: 4-phenyl-1-butyne (1.0 mmol, 130 mg), **2** (0.01 mmol, 19.7 mg), AgOTf (0.02 mmol, 5.1 mg), toluene (1.0 mL). [b] Isolated yields as a mixture of **3a** and **3b**. [c] Molar ratios determined by ¹H NMR spectroscopy on the isomeric mixtures after purification.

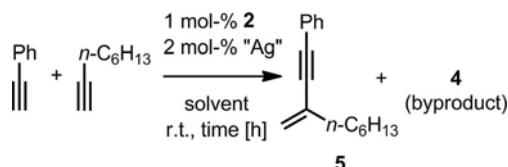
Next, we evaluated the reactivity of 1-octyne and ethynylbenzene (Scheme 4). 1-Octyne was converted almost exclusively into terminal alkene **4** in 83 % yield. In the case of ethynylbenzene, virtually no reaction took place.



Scheme 4. Reactivities of (a) 1-octyne and (b) ethynylbenzene.

With these few examples completed we were able to begin a search for a possible selective cross-dimerization. We were excited to find that ethynylbenzene and 1-octyne were preferentially coupled to give cross-dimer **5**^[19] as the predominant product in 47 % yield (Scheme 5 and Table 2, Entry 1). A homo-dimer was also formed under the reaction conditions but only fractionally so (ratio **5/4** = 5.4:1). To absolutely confirm the structure, we reduced **5** to (3-methylnonyl)benzene **6** in 82 %

(Scheme 6) and, notably, two benzylic protons [δ = 2.61 ppm, triplet, in CDCl₃] were identified. It is likely that ethynylbenzene plays the role of an electron-donor to an activated 1-octyne that becomes an electron-acceptor. For reaction conditions with CH₂Cl₂ and mesitylene only **5** was predominantly generated, and the use of THF failed to produce anything (Table 2, Entries 2–4). Various silver sources were also examined as reaction components (Table 2, Entries 5–8); AgBF₄ and AgNTf₂ proved quite promising. As shown in Table 2, Entry 9, the formation of **5** was improved to 62 % yield^[20] when the quantity of 1-octyne was increased to 1.5 equiv.

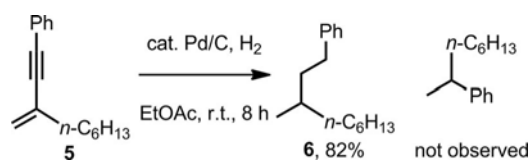


Scheme 5. Cavitand **2** catalyzed cross-dimerization.

Table 2. Cross-dimerization conducted according to Scheme 5.^[a]

Entry	Solvent	Ag source	Yield of 5 [%] ^[b]	Ratio of 5/4 ^[c]
1	toluene	AgOTf	47	5.4:1
2	CH ₂ Cl ₂	AgOTf	36	3.6:1
3	mesitylene	AgOTf	32	4.3:1
4	THF	AgOTf	0	–
5	toluene	AgBF ₄	49	3.3:1
6	toluene	AgSbF ₆	17	3.6:1
7	toluene	AgNO ₃	0	–
8	toluene	AgNTf ₂ ^[d]	51	3.1:1
9	toluene	AgOTf ^[d]	62	3.4:1

[a] Conditions: ethynylbenzene (1 mmol, 102 mg), 1-octyne (1.2 mmol, 132 mg), **2** (0.01 mmol, 19.7 mg), Ag source (0.02 mmol), solvent (1 mL), reaction time 20 h. [b] Isolated yields after purification by silica-gel column chromatography. [c] Molar ratios determined by ¹H NMR spectroscopy of the crude products. [d] 1.5 mmol of 1-octyne was used.



Scheme 6. Structural elucidation of **5** by reduction to **6**.

Using these initially optimized conditions, we explored further optimization possibilities. Time and concentration were examined (Table 3). Decreasing concentration had a negative effect (Table 3, Entries 1, 3, and 5), whereas prolonged reaction times increased yields, surprisingly at all concentrations to 62–70 % (Table 3, Entries 2, 4, and 6). Reaction conditions described for Table 3, Entry 4 afforded **5** in the highest yield of 70 % using a 4.1:1 molar ratio of **5/4**.

We again conducted thorough control experiments: (1) utilizing the mono-gold complex^[9] shown in panel (a) of Scheme 1, (2) using commercially available AuCl·PPh₃, (3) using phosphorus-free AuCl·S(CH₃)₂, and (4) using the gold-free host **1**. Dimers were not observed in any case. Thus, the substructure of dinuclear Au complex **2** is indispensable for producing cross-dimer **5**. At this time, treatment of **2** with silver could reason-

Table 3. Evaluation of substrate concentrations in cross-dimerization reactions shown in Scheme 5.^[a]

Entry	Amount of toluene [mL]	Time [h]	Yield of 5 [%] ^[b]	Ratio of 5/4 ^[c]
1	1	2	47	2.8:1
2	1	20	62	3.4:1
3	5	2	31	2.9:1
4	5	20	70	4.1:1
5	10	2	25	3.4:1
6	10	20	62	2.5:1

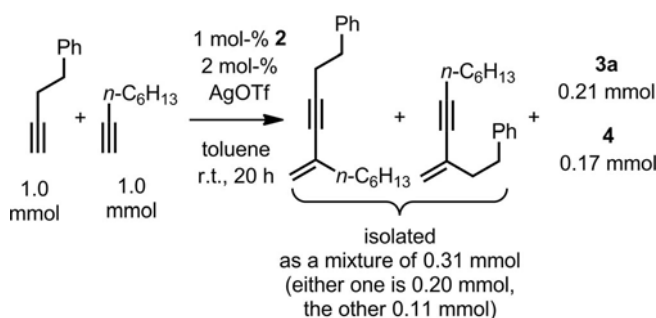
[a] Conditions: ethynylbenzene (1 mmol, 102 mg), 1-octyne (1.5 mmol, 165 mg), **2** (0.01 mmol, 19.7 mg), AgOTf (0.02 mmol, 5.1 mg). [b] Isolated yields after purification by silica-gel column chromatography. [c] Molar ratios determined by ¹H NMR spectroscopy of the crude products.

ably result in either a monocationic or dicationic gold complex; these details require further treatment at a future time to develop a complete understanding of the system.

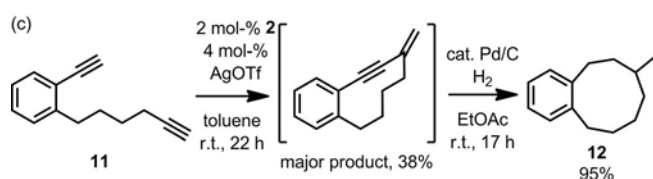
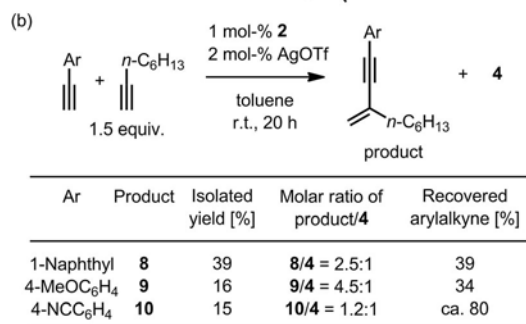
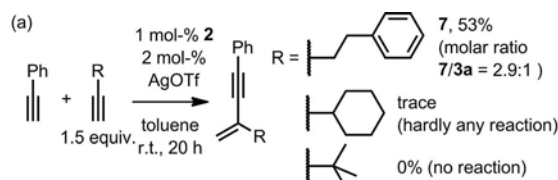
Other alkyne pairs were tested for hetero-dimerization. As illustrated in panel (a) of Scheme 7, the alkylalkyne partner needs a CH₂ group adjacent to the triple bond; for instance, phenylethyl species **7** gave the hetero-dimer in 53 % yield. For ethynylcyclohexane and *tert*-butylalkyne, neither hetero- nor homo-dimers were generated, and almost all the starting ethynylbenzene remained. In part (b), arylalkyne substituents were added as potential partners for 1-octyne. The yields of naphthyl species **8**, methoxy species **9**,^[21] and nitrile species **10** were 39 %, 16 %, and 15 %, respectively. In all three cases the hetero-adducts predominate over homo-dimer **4**. Notably too, is that excess starting arylalkynes, remained unreacted.^[22] In panel (c), we were happy to find that intramolecular cyclization of diyne **11** proceeded to give highly strained enyne in 38 % yield as a major product. The very labile enyne was converted into nine-membered ring **12** in 95 % yield. However, this catalytic system lacks substrate generality; product scope was unfortunately nar-

row, internal alkynes failed to undergo reaction, and high-yielding transformations were not achieved.

The reaction between 4-phenyl-1-butyne and 1-octyne gave inseparable mixtures of two hetero-adducts and homo-adducts **3a** and **4** (Scheme 8). This result is not surprising. Nevertheless, the combination of C₆H₅–CCH and R–CH₂CCH (for example, Table 3, Entry 4) is an exquisite pair for selective formation of hetero-adducts in high yields. Such specificity is the rule in enzymatic reactions, where precise combinations are the rule. From the viewpoint of molecular recognition, cavitand **2** might resemble enzymes more closely than we had originally envisaged.^[23] Future cavitands might allow greater discrimination based on the size of substrates, whereas **2** seems to remain governed by electronics of the hetero-partners.



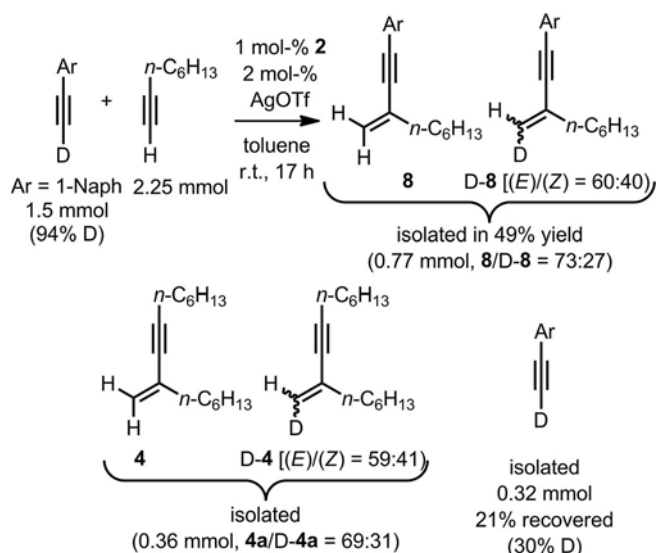
Scheme 8. Dimerization between 4-phenyl-1-butyne and 1-octyne.



Scheme 7. Cross-dimerization between: (a) ethynylbenzene and alkylalkyne, (b) arylalkyne and 1-octyne, (c) intramolecular aryl- and alkylalkyne.

A preliminary mechanistic investigation was performed using a deuterium-labeled terminal alkyne (Scheme 9). The dimerization utilizing a 94 % D-labeled alkyne yielded a very complex mixture. Hetero-**8** and D-containing-**8** were isolated in 49 % with a 73:27 ratio.^[24] The reaction also afforded homo-**4** and homo-D-containing-**4** with a 69:31 ratio. The recovered starting alkyne (21 %) lost a significant fraction of the D-label in the process, retaining only 30 % of the original D-label. In addition, the balance of deuterium did not agree between the 1-(D-ethynyl)naphthalene and the deuterated products; ca. 70 % of the total deuterium labels were gone. Given the observed shuffle of deuterium, we consider that bis-Au compound **2** abstracted both the alkynyl deuterium and alkyl proton to attach anew, followed by generation of 1-ethynyl-naphthalene and D-labelled oct-1-yne, and dimerization between those alkynes to give **8**, D-containing-**8**, **4**, and D-containing **4**.

Thus, a primitive cycle for catalytic dimerization might be depicted as in Figure 2. We envision that, initially, **2** reacts with



Scheme 9. Cross-dimerization utilizing 1-(D-ethynyl)naphthalene.

AgOTf to yield the bis-Au cation species; the Lewis-acidic species would selectively recognize a pair of alkyne triple bonds. The molecular recognition tends to prefer ethynylbenzene and 1-octyne to two 1-octynes presumably due to steric and/or electronic reasons, although the mechanism resulting in the selectivity is not yet fully understood. Then, the deprotonation step gives an Au acetylide, taking a TfOH in and out; this step would be reversible since the experiment in Scheme 9 revealed

deuterium shuffling. Finally, C–C bond formation through dimerization occurs and is followed by the generation of cross-dimer **5** (R = Ph) and homo-dimer **4** (R = C₆H₁₃) along with the regeneration of the first bis-Au cation.

The obvious complexity of this system, including activation with Ag to give a bis-Au cation species^[25] that couples two reaction partners, leaves most of the mechanistic aspects open to further exploration. In this work our major interest was, first and foremost, on new capabilities. Both metal centers can be tuned by alteration of the P ligand, and both walls can be modified, perhaps through lengthening to further limit what can enter – or perhaps what types of intermediates can be stabilized. Such further efforts will clearly require extensive study and careful planning.

Conclusions

The synthesis and characterization of a doubly, inwardly directed AuCl-cavitand stands alone in the area of supramolecular chemistry and has only a few parallels in the synthetic realm. Natural examples of systems containing several catalytic sites where two or more metals carry out surprising reactions do exist. In this work, when ionized by treatment with Ag, a bis-Au cavitand (**2**) displays efficient chemical reactivity as it selectively dimerizes two terminal alkynes. With **2**, an intermolecular dimerization takes place even where a path to an intramolecular product clearly should exist. This catalyst can be used to carry out homo-dimerization as well as hetero-dimerization reactions, and the latter can be done selectively with correct pairing of

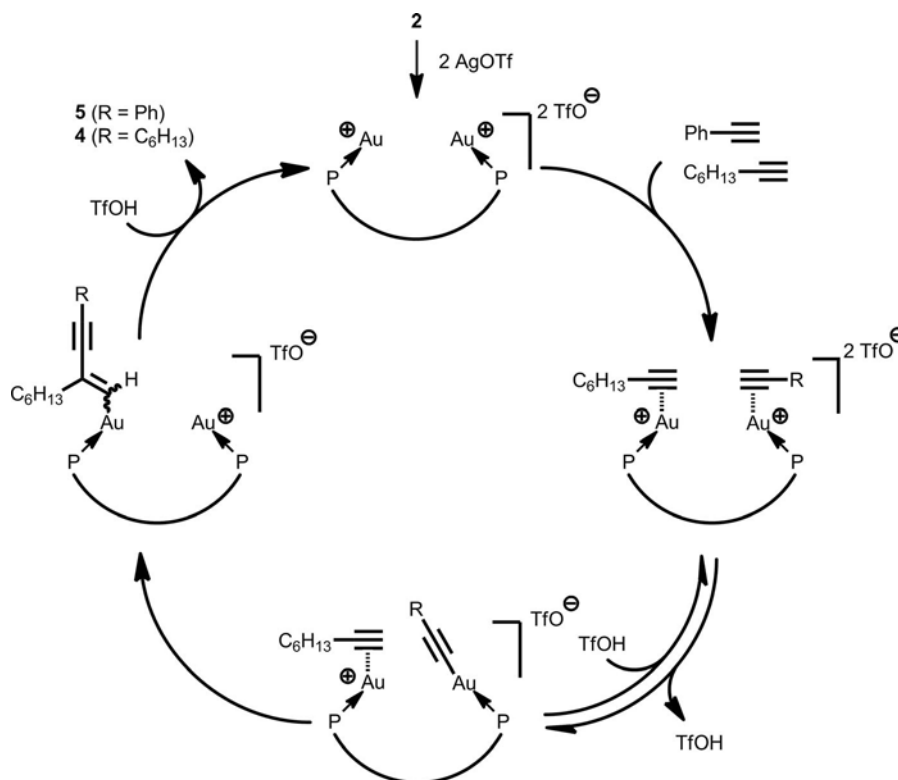


Figure 2. Plausible catalytic cycle for the **2**-promoted dimerization reaction.

alkynes. Although yields remain modest, the presence of two metal centers in the confined space allows us to achieve potent chemical transformations. Development of a deeper understanding of how this system works and of new catalytic transformations and new cavitands begins now.

Experimental Section

Gram-Scale Synthesis of Bis-Au Complex 2: Under N₂, a solution of **1**^[14] (1.05 g, 0.70 mmol) in toluene (14 mL) underwent addition of AuCl·S(CH₃)₂ (432 mg, 1.68 mmol), and the mixture was stirred for 30 min with confirmation that **1** had disappeared by TLC monitoring. After all the volatiles had been evaporated, the crude products were purified by short-plugged silica-gel column chromatography (eluent: hexane/EtOAc, 2:1) to afford 1.33 g of **2** as white powder materials in 96 % yield. ¹H NMR (400 MHz, CDCl₃): δ = 7.90 (dd, *J* = 6.4, 3.4 Hz, 4 H), 7.58 (dd, *J* = 6.4, 3.4 Hz, 4 H), 7.410–7.406 (m, 4 H), 7.23 (s, 4 H), 5.73 (t, *J* = 8.2 Hz, 2 H), 4.58–4.55 (m, 2 H), 3.10 (d, ³J_{PH} = 13.1 Hz, 12 H), 2.33–2.32 (m, 4 H), 2.21–2.19 (m, 4 H), 1.42–1.27 (m, 72 H), 0.91–0.86 (m, 12 H) ppm. ¹³C NMR (100 MHz, CDCl₃): δ = 153.1, 152.0, 146.2 (d, *J*_{CP} = 6.0 Hz), 140.1, 136.6, 135.9 (d, *J*_{CP} = 2.4 Hz), 130.3, 128.7, 122.8, 117.9 (d, *J*_{CP} = 3.8 Hz), 36.9 (d, *J*_{CP} = 11.7 Hz), 35.8, 34.1, 32.7, 32.2, 30.5, 30.0, 29.7, 28.2, 23.0, 14.4 ppm. ³¹P NMR (162 MHz, CDCl₃): δ = 111.9 ppm. MS (MALDI-TOF): *m/z* = 1932 [M – Cl]⁺. IR (neat): $\tilde{\nu}$ = 2921, 2850, 1482, 1402, 1329, 1271, 1065, 989 cm^{−1}. HRMS (MALDI-TOF): calcd. for C₉₂H₁₂₄Au₂ClN₆O₈P₂ [M – Cl]⁺ 1931.7975, found 1931.8026.

Synthesis of 3a, 3b, and 3c: Scheme 3, and Table 1, Entry 2. Under N₂, **2** (30 mg, 0.015 mmol) in a 20 mL Schlenk tube was dissolved in dry toluene (1.5 mL), and AgOTf (7.7 mg, 0.03 mmol) was added at room temperature. After 5 min of stirring, 4-phenyl-1-butyne (0.21 mL, 1.5 mmol) was added, and the reaction was monitored by TLC for 24 h. The solvent was evaporated to give 240 mg of crude product as a dark brown oil. Purification by short-plugged silica-gel column chromatography afforded an isomeric mixture of **3a** and **3b** (NMR yields: 71 % and 2 %, respectively; actually, we laboriously separated them in small amounts for taking NMR spectra, but both were too labile to keep pure forms). Data for **3a**: ¹H NMR (400 MHz, CDCl₃): δ = 7.32–7.16 (m, 10 H), 5.21 (s, 1 H), 5.10 (s, 1 H), 2.88 (t, *J* = 7.5 Hz, 2 H), 2.78 (t, *J* = 7.5 Hz, 2 H), 2.64 (t, *J* = 7.5 Hz, 2 H), 2.40 (t, *J* = 7.5 Hz, 2 H) ppm. ¹³C NMR (100 MHz, CDCl₃): δ = 141.9, 141.0, 131.6, 128.83, 128.82, 128.7, 128.6, 126.6, 126.2, 120.7, 90.0, 81.8, 39.7, 35.5, 34.9, 21.8 ppm. MS (DI): *m/z* = 260 [M]⁺. IR (neat): $\tilde{\nu}$ = 3060, 3026, 2924, 2858, 1803, 1604, 1495, 1452, 1338, 1076, 1030, 897, 698 cm^{−1}. HRMS (DART): calcd. for C₂₀H₂₁ [M + H]⁺ 261.1638, found 261.1614. Data for **3b**: ¹H NMR (400 MHz, CDCl₃): δ = 7.31–7.17 (m, 10 H), 5.73 (t, *J* = 7.4 Hz, 1 H), 3.51 (d, *J* = 7.4 Hz, 2 H), 2.89 (t, *J* = 7.4 Hz, 2 H), 2.69 (t, *J* = 7.4 Hz, 2 H), 1.85 (s, 3 H) ppm. ¹³C NMR (100 MHz, CDCl₃): δ = 141.1, 141.0, 135.1, 128.85, 128.79, 128.72, 128.68, 126.6, 126.2, 119.4, 93.3, 81.0, 37.2, 35.6, 23.7, 22.0 ppm. To one-neck flask charged with an isomeric mixture of **3a** and **3b** (117 mg, 0.45 mmol) under H₂ were added EtOAc (1 mL) and Pd/C (12 mg, 10 wt.-%). After stirring for 8 h, the reaction mixture was filtered through a pad of Celite, and the filtrate was concentrated in vacuo to give a mixture of yellow oil and white solid. Purification by silica-gel column chromatography (eluent: hexane only) afforded **3c** of 107 mg (89 %) as a pale yellow oil. ¹H NMR (400 MHz, CDCl₃): δ = 7.29–7.25 (m, 4 H), 7.18–7.16 (m, 6 H), 2.68–2.51 (m, 4 H), 1.65–1.54 (m, 3 H), 1.44–1.16 (m, 6 H), 0.92 (d, *J* = 14.7 Hz, 3 H) ppm. ¹³C NMR (100 MHz, CDCl₃): δ = 143.4, 143.2, 128.72, 128.69, 128.58, 128.56, 125.90, 125.87, 39.3, 37.0, 36.3, 33.8, 32.7, 32.1, 27.0, 19.9 ppm. MS (DI): *m/z* = 266 [M]⁺. IR (neat): $\tilde{\nu}$ =

3061, 2926, 2854, 1604, 1495, 1453, 1030, 742, 695 cm^{−1}. C₂₀H₂₆ (266.43): calcd. C 90.16, H 9.84; found C 90.15, H 9.83.

Synthesis of 5: Table 3, Entry 4. Under N₂, **2** (20 mg, 0.010 mmol) was dissolved in dry toluene (5 mL), and AgOTf (5.1 mg, 0.02 mmol) was added at room temperature. After 5 min of stirring, the ethynylbenzene (102 mg, 1.0 mmol) and 1-octyne (165 mg, 1.5 mmol) were added, and the reaction was conducted for 20 h. The solvent was evaporated to give a crude product, and the following purification by silica-gel column chromatography (hexane only) afforded 149 mg of **5** in 70 % yield as a yellow oil. ¹H NMR (400 MHz, CDCl₃): δ = 7.44–7.42 (m, 2 H), 7.33–7.29 (m, 3 H), 5.40 (d, *J* = 2.0 Hz, 1 H), 5.29 (d, *J* = 2.0 Hz, 1 H), 2.24 (t, *J* = 7.5 Hz, 2 H), 1.59 (tt, *J* = 7.5, 7.5 Hz, 2 H), 1.38–1.26 (m, 6 H), 0.89 (t, *J* = 7.1 Hz, 3 H) ppm. ¹³C NMR (100 MHz, CDCl₃): δ = 132.2, 131.9, 128.6, 128.4, 123.7, 121.3, 90.3, 89.4, 37.6, 32.0, 29.0, 28.5, 23.0, 14.4 ppm. MS (DI): *m/z* = 212 [M]⁺, 142 [M + H – C₅H₁₁]⁺. IR (neat): $\tilde{\nu}$ = 2925, 2854, 1799, 1608, 1442, 1306, 895, 752 cm^{−1}. HRMS (DART): calcd. for C₁₆H₂₁ [M + H]⁺ 213.1638, found 213.1610.

Synthesis of 12: Scheme 7 (c). Under N₂, **2** (47 mg, 0.024 mmol) was dissolved in dry toluene (12 mL), and AgOTf (12 mg, 0.048 mmol) was added at room temperature. After 5 min of stirring, diyne **11** (220 mg, 1.2 mmol) was added and the reaction was conducted for 22 h. The solvent was evaporated to give a crude product, and the following purification by silica-gel column chromatography (hexane only) afforded the corresponding enyne (83 mg) in 38 % yield as a white oil; right after the purification, the enyne turned into a yellow oil, and the NMR spectra revealed the distorted nine-membered enyne was fragile. ¹H NMR (400 MHz, CDCl₃): δ = 7.28–7.15 (m, 4 H), 5.19 (s, 2 H), 2.81 (t, *J* = 6.7 Hz, 2 H) 2.57 (t, *J* = 5.9 Hz, 2 H), 1.93 (tt, *J* = 6.7, 6.7 Hz, 2 H), 1.82 (tt, *J* = 5.9, 5.9 Hz, 2 H) ppm. ¹³C NMR (100 MHz, CDCl₃): δ = 148.7, 132.2, 129.2, 128.5, 128.3, 126.4, 123.7, 117.3, 103.4, 97.2, 36.9, 34.8, 29.3, 27.3 ppm. MS (LCMS-IT-TOF): *m/z* = 183 [M + H]⁺. IR (neat): $\tilde{\nu}$ = 3063, 2921, 2850, 1614, 1454, 893, 751 cm^{−1}. HRMS (DART): calcd. for C₁₄H₁₅ [M + H]⁺ 183.1168, found 183.1164. Thus, the freshly prepared enyne was provided to the next reduction step for the structural elucidation. To the flask charged with the enyne (19 mg, 0.10 mmol) in EtOAc (0.3 mL) under H₂ was added a catalytic amount of 10 % Pd/C (2 mg), and the mixture was stirred at room temperature for 17 h. After the mixture had been filtered through a pad of Celite, the filtrate was concentrated in vacuo to give a colorless oil of **12** in pure form (18 mg, 95 % yield). ¹H NMR (400 MHz, CDCl₃): δ = 7.14–7.07 (m, 4 H), 2.90–2.62 (m, 4 H), 1.93–1.84 (m, 1 H), 1.75 (dt, *J* = 11, 3.8 Hz, 1 H) 1.56–1.26 (m, 7 H), 0.83 (d, *J* = 6.3 Hz, 3 H) ppm. ¹³C NMR (100 MHz, CDCl₃): δ = 142.8, 141.6, 130.1, 129.9, 126.4, 126.3, 38.0, 35.0, 32.4, 31.2, 30.7, 30.0, 24.7, 23.5 ppm. MS (LCMS-IT-TOF): *m/z* = 189 [M + H]⁺. IR (neat): $\tilde{\nu}$ = 2921, 2866, 1450, 749 cm^{−1}. HRMS (DART): calcd. for C₁₄H₂₁ [M + H]⁺ 189.1638, found 189.1632.

9-Methylenepentadec-7-yne (4): Yellow oil. ¹H NMR (400 MHz, CDCl₃): δ = 5.19 (d, *J* = 1.5 Hz, 1 H), 5.11 (d, *J* = 1.5 Hz, 1 H), 2.30 (t, *J* = 7.0 Hz, 2 H), 2.11 (t, *J* = 7.5 Hz, 2 H), 1.56–1.24 (m, 16 H), 0.91–0.87 (m, 6 H) ppm. ¹³C NMR (100 MHz, CDCl₃): δ = 132.8, 119.6, 90.4, 81.4, 30.8, 32.0, 31.7, 29.1, 29.0, 28.9, 28.4, 23.0, 22.9, 19.6, 14.42, 14.38 ppm. MS (DI): *m/z* = 135 [M + H – C₆H₁₃]⁺, 220 [M]⁺. IR (neat): $\tilde{\nu}$ = 2927, 2856, 1610, 1462, 1379, 891, 725 cm^{−1}. HRMS (DART): calcd. for C₁₆H₂₉ [M + H]⁺ 221.2264, found 221.2236.

(3-Methylnonyl)benzene (6): ¹H NMR (400 MHz, CDCl₃): δ = 7.29–7.26 (m, 2 H), 7.19–7.15 (m, 3 H), 2.69–2.52 (m, 2 H), 1.68–1.58 (m, 1 H), 1.46–1.15 (m, 12 H), 0.92 (d, *J* = 5.8 Hz, 3 H), 0.89 (t, *J* = 7.2 Hz, 3 H) ppm. ¹³C NMR (100 MHz, CDCl₃): δ = 143.6, 128.7, 128.6, 125.9, 39.3, 37.3, 33.9, 32.9, 32.3, 30.0, 27.3, 23.1, 20.0, 14.5 ppm. MS (DI): *m/z* = 218 [M]⁺. IR (neat): $\tilde{\nu}$ = 3027, 2954, 2923, 2854, 1496, 1455,

1377, 1031, 743, 696 cm⁻¹. C₁₆H₂₆ (218.38): calcd. C 88.00, H 12.00; found C 88.07, H 12.31.

(3-Methylenepent-1-yne-1,5-diyl)dibenzene (7): Yellowish white oil. ¹H NMR (400 MHz, CDCl₃): δ = 7.48–7.46 (m, 2 H), 7.35–7.18 (m, 8 H), 5.42 (d, *J* = 1.7 Hz, 1 H), 5.27 (d, *J* = 1.7 Hz, 1 H), 2.93 (t, *J* = 7.9 Hz, 2 H), 2.56 (t, *J* = 7.9 Hz, 2 H) ppm. ¹³C NMR (100 MHz, CDCl₃): δ = 141.7, 131.9, 131.2, 128.8, 128.62, 128.61, 128.5, 126.2, 123.5, 122.1, 90.0, 89.9, 39.4, 34.9 ppm. MS (DI): *m/z* = 232 [M]⁺. IR (neat): $\tilde{\nu}$ = 3026, 2922, 2856, 1946, 1803, 1491, 1306, 897, 750, 688 cm⁻¹. HRMS (DART): calcd. for C₁₈H₁₇ [M + H]⁺ 233.1325, found 233.1296.

1-(3-Methylenenon-1-ynyl)naphthalene (8): Colorless oil. ¹H NMR (400 MHz, CDCl₃): δ = 8.34 (d, *J* = 8.3 Hz, 1 H), 7.85 (d, *J* = 8.0 Hz, 1 H), 7.82 (d, *J* = 8.0 Hz, 1 H), 7.68 (d, *J* = 7.1 Hz, 1 H), 7.57 (dd, *J* = 8.3, 8.3 Hz, 1 H), 7.52 (dd, *J* = 8.3, 8.3 Hz, 1 H), 7.43 (dd, *J* = 8.0, 8.0 Hz, 1 H), 5.53 (d, *J* = 1.2 Hz, 1 H), 5.37 (d, *J* = 1.2 Hz, 1 H), 2.35 (t, *J* = 7.5 Hz, 2 H), 1.69 (tt, *J* = 7.5, 7.5 Hz, 2 H), 1.42–1.32 (m, 6 H), 0.91 (t, *J* = 6.8 Hz, 3 H) ppm. ¹³C NMR (100 MHz, CDCl₃): δ = 133.6, 133.5, 132.4, 130.6, 128.9, 128.6, 127.0, 126.7, 126.5, 125.5, 121.5, 121.4, 95.3, 87.6, 37.7, 32.0, 29.0, 28.6, 23.0, 14.5 ppm. MS (LCMS-IT-TOF): *m/z* = 263 [M + H]⁺. IR (neat): $\tilde{\nu}$ = 3057, 2925, 2854, 1604, 1460, 1396, 1304, 895, 796, 769 cm⁻¹. HRMS (DART): calcd. for C₂₀H₂₃ [M + H]⁺ 263.1794, found 263.1766.

1-Methoxy-4-(3-methylenenon-1-ynyl)benzene (9): Pale yellow oil. ¹H NMR (400 MHz, CDCl₃): δ = 7.38 (d, *J* = 8.3 Hz, 2 H), 6.84 (d, *J* = 8.3 Hz, 2 H), 6.10 (d, *J* = 1.1 Hz, 1 H), 5.25 (d, *J* = 1.1 Hz, 1 H), 3.81 (s, 3 H), 2.23 (t, *J* = 7.5 Hz, 2 H), 1.58 (tt, *J* = 7.5, 7.5 Hz, 2 H), 1.38–1.25 (m, 6 H), 0.89 (t, *J* = 6.7 Hz, 3 H) ppm. ¹³C NMR (100 MHz, CDCl₃): δ = 159.8, 133.3, 132.4, 120.6, 115.9, 114.2, 89.4, 89.0, 55.6, 37.7, 32.0, 29.0, 28.5, 23.0, 14.4 ppm. MS (LCMS-IT-TOF): *m/z* = 243 [M + H]⁺. IR (neat): $\tilde{\nu}$ = 2927, 2854, 1601, 1508, 1286, 1246, 1169, 1032, 893, 829 cm⁻¹. HRMS (DART): calcd. for C₁₇H₂₃O [M + H]⁺ 243.1743, found 243.1717.

4-(3-Methylenenon-1-ynyl)benzonitrile (10): Whitish yellow oil. ¹H NMR (400 MHz, CDCl₃): δ = 7.55 (d, *J* = 8.6 Hz, 2 H), 7.51 (d, *J* = 8.6 Hz, 2 H), 5.47 (d, *J* = 1.7 Hz, 1 H), 5.38 (d, *J* = 1.7 Hz, 1 H), 2.24 (t, *J* = 7.5 Hz, 2 H), 1.55 (tt, *J* = 7.5, 7.5 Hz, 2 H), 1.38–1.25 (m, 6 H), 0.89 (t, *J* = 6.8 Hz, 3 H) ppm. ¹³C NMR (100 MHz, CDCl₃): δ = 132.4, 132.3, 131.6, 128.7, 123.1, 118.8, 111.6, 94.7, 87.7, 37.2, 31.9, 28.9, 28.4, 22.9, 14.4 ppm. MS (LCMS-IT-TOF): *m/z* = 238 [M + H]⁺. IR (neat): $\tilde{\nu}$ = 2925, 2856, 2227, 1606, 1500, 903, 837, 552 cm⁻¹. HRMS (DART): calcd. for C₁₇H₂₀N [M + H]⁺ 238.1590, found 238.1582.

Acknowledgments

We thank the Japan Society for the Promotion of Science Invitation Fellowships for Research in Japan (long-term, L-15528, M. P. S). The authors thank Dr. Seiji Watase, Dr. Toshiyuki Iwai and Dr. Takatoshi Ito at OMTRI for assistance with X-ray diffraction and scattering data acquisitions and HRMS. Dr. Kiyosei Takasu, Dr. Ken-ichi Yamada, and Dr. Yosuke Yamaoka are gratefully thanked for assistance with mass spectrometer operations.

Keywords: Introverted functionality · Cavitands · Supramolecular catalysis · Caged molecule · Molecular recognition · Alkynes · Chemoselectivity

- [1] a) J. A. Gerlt, *Chem. Rev.* **1987**, 87, 1079–1105; b) G. Varani, *Annu. Rev. Biophys. Biomol. Struct.* **1995**, 24, 379–404; c) M. V. Rodnina, W. Wintermeyer, *Curr. Opin. Struct. Biol.* **2003**, 13, 334–340; d) K. Shen, A. C. Hines,

D. Schwarzer, K. A. Pickin, P. A. Cole, *Biochim. Biophys. Acta Proteins Proteomics* **2005**, 1754, 65–78.

- [2] a) F. A. Tezcan, J. T. Kaiser, D. Mustafi, M. Y. Walton, J. B. Haward, D. C. Rees, *Science* **2005**, 309, 1377–1380; b) T. Spatzal, M. Aksoyoglu, L. Zhang, S. L. A. Andrade, E. Schleicher, S. Weber, D. C. Rees, O. Einsle, *Science* **2011**, 334, 940; c) K. M. Lancaster, M. Roemelt, P. Ettenhuber, Y. Hu, M. W. Ribbe, F. Neese, U. Bergmann, S. DeBeer, *Science* **2011**, 974–977.
- [3] a) A. J. Skerra, *J. Mol. Recognit.* **2000**, 13, 167–187; b) G. Folkers, C. D. P. Klein, *Angew. Chem. Int. Ed.* **2001**, 40, 4175–4177–4305; *Angew. Chem.* **2001**, 113, 4303; c) C. Khosla, P. B. Harbury, *Nature* **2001**, 409, 247–252; d) T. C. Bruice, *Acc. Chem. Res.* **2002**, 35, 139–148.
- [4] a) J. Rebek Jr., *J. Org. Chem.* **2004**, 69, 2651–2660; b) J. Rebek Jr., *Nature* **2006**, 444, 557.
- [5] a) J. R. Moran, S. Karbach, D. J. Cram, *J. Am. Chem. Soc.* **1982**, 104, 5826–5828; b) D. J. Cram, *Science* **1983**, 219, 1177–1183; c) J. R. Moran, J. L. Ericson, E. Dalcanele, J. A. Bryant, C. B. Knobler, D. J. Cram, *J. Am. Chem. Soc.* **1991**, 113, 5707–5714; d) D. J. Cram, J. M. Cram, *Container Molecules and Their Guests*, Royal Society of Chemistry, Cambridge, **1994**, pp. 85–130.
- [6] a) A. R. Renslo, J. Rebek Jr., *Angew. Chem. Int. Ed.* **2000**, 39, 3281–3283; *Angew. Chem.* **2000**, 112, 3419; b) P. L. Wash, A. R. Renslo, J. Rebek Jr., *Angew. Chem. Int. Ed.* **2001**, 40, 1221–1222; *Angew. Chem.* **2001**, 113, 1261; c) T. Iwasawa, R. J. Hooley, J. Rebek Jr., *Science* **2007**, 317, 493–496.
- [7] a) S. R. Shenoy, F. R. Pinacho Crisostomo, T. Iwasawa, J. Rebek Jr., *J. Am. Chem. Soc.* **2008**, 130, 5658–5659; b) F. R. Pinacho Crisostomo, A. Lledo, S. R. Shenoy, T. Iwasawa, J. Rebek Jr., *J. Am. Chem. Soc.* **2009**, 131, 7402–7410.
- [8] a) Z. J. Wang, K. N. Clary, R. G. Bergman, K. N. Raymond, F. D. Toste, *Nature Chem.* **2013**, 5, 100–103; b) M. Raynal, P. Ballester, A. Vidal-Ferran, P. W. N. M. van Leeuwen, *Chem. Soc. Rev.* **2014**, 43, 1660–1733; c) M. Raynal, P. Ballester, A. Vidal-Ferran, P. W. N. M. van Leeuwen, *Chem. Soc. Rev.* **2014**, 43, 1734–1787; d) S. Mosca, Y. Yu, J. V. Gavette, K.-D. Zhang, J. Rebek Jr., *J. Am. Chem. Soc.* **2015**, 137, 14582–14583.
- [9] M. P. Schramm, M. Kanaura, K. Ito, M. Ide, T. Iwasawa, *Eur. J. Org. Chem.* **2016**, 813–820.
- [10] a) M. Kanaura, K. Ito, M. P. Schramm, D. Ajami, T. Iwasawa, *Tetrahedron Lett.* **2015**, 56, 4824–4828; b) K. Ohashi, K. Ito, T. Iwasawa, *Eur. J. Org. Chem.* **2014**, 1597–1601.
- [11] C. Gibson, J. Rebek Jr., *Org. Lett.* **2002**, 4, 1887–1890.
- [12] a) M. Mettry, M. P. Moehlig, R. J. Hooley, *Org. Lett.* **2015**, 17, 1497–1500; b) N. Khiri, E. Bertrand, M.-J. Ondel-Eymin, Y. Rousselin, J. Bayardon, P. D. Harvey, S. Juge, *Organometallics* **2010**, 29, 3622–3631; c) H. El Moll, D. Semeril, D. Matt, L. Toupet, *Adv. Synth. Catal.* **2010**, 352, 901–908; d) Z. R. Laughrey, B. C. Gibb, *J. Org. Chem.* **2006**, 71, 1289–1294; e) L. Poorters, D. Armspach, D. Matt, L. Toupet, P. G. Jones, *Angew. Chem. Int. Ed.* **2007**, 46, 2717–2719; *Angew. Chem.* **2007**, 119, 2773.
- [13] a) D. Semeril, D. Matt, *Coord. Chem. Rev.* **2014**, 279, 58–95; b) S. H. A. M. Leenders, R. Gramage-Doria, B. de Bruin, J. N. H. Reek, *Chem. Soc. Rev.* **2014**, 44, 433–448; c) C. Jeunesse, D. Armspach, D. Matt, *Chem. Commun.* **2005**, 5603–5614.
- [14] T. Iwasawa, T. Kamei, K. Hama, Y. Nishimoto, M. Nishiuchi, Y. Kawamura, *Tetrahedron Lett.* **2008**, 49, 4758–4762.
- [15] Compound **2**: Triclinic, space group P121/c1, colorless, *a* = 34.6027(9) Å, *b* = 12.1512(3) Å, *c* = 23.7440(7) Å, β = 110°, *V* = 9369.0(4) Å³, *Z* = 4, *T* = 173 K, *d*_{calcd} = 1.456 g cm⁻³, μ(Mo-Kα) = 3.3433 mm⁻¹, *R*₁ = 0.0584, *wR*₂ = 0.1596, GOF = 1.046. CCDC 1411464 (for **2**) contains the supplementary crystallographic data for this paper. These data can be obtained free of charge from The Cambridge Crystallographic Data Centre.
- [16] The ORTEP drawing of **2**·CH₂Cl₂ is shown in the Supporting Information.
- [17] a) J. M. Conia, P. Le Perche, *Synthesis* **1975**, 1–19; b) J. J. Kennedy-Smith, S. T. Staben, F. D. Toste, *J. Am. Chem. Soc.* **2004**, 126, 4526–4527.
- [18] Complete details are in the Supporting Information.
- [19] To the best of our knowledge, selective cross-dimerization of two different terminal alkynes for producing the head-to-tail-fashioned enynes are reported by only two groups; one uses an Rh catalyst and the other uses Pd, see: a) H.-D. Xu, R.-W. Zhang, X. Li, S. Huang, W. Tang, W.-H. Hu, *Org. Lett.* **2013**, 15, 840–843; b) N. Tuskada, S. Ninomiya, Y. Aoyama, Y. Inoue, *Pure Appl. Chem.* **2008**, 80, 1161–1166.
- [20] In Tables 2 and 3, the starting alkynes remained somewhat unreacted.

- [21] Compound **9** was lost during the purification on silica-gel column chromatography.
- [22] Structure elucidations for **4** and **7–10** were facilitated by the reduction in Scheme 5. These data are listed in the Supporting Information.
- [23] J. Rebek Jr., in *Hydrogen-bonded Capsules*, World Scientific Publishing Co. Pte Ltd., Imperial College Press, UK, **2016**, pp. 191–216.
- [24] The presence of *exo*-[D₂]methylene products for **8** and **4** was evaluated, but not verified by ¹H NMR spectra.
- [25] M. T. Reetz, K. Sommer, *Eur. J. Org. Chem.* **2003**, 3485–3496.

Received: March 23, 2016
Published Online: April 24, 2016